

## METAL MICROMECHANICAL FILTER-POWER AMPLIFIER UTILIZING A DISPLACEMENT-AMPLIFYING RESONANT SWITCH

Wei-Chang Li, Yang Lin, and Clark T.-C. Nguyen

Dept. of EECS, University of California at Berkeley, Berkeley, California, USA

### ABSTRACT

Power gain up to 13.8 dB has been generated by a 23-MHz switched-mode power amplifier circuit employing an Al metal micromechanical slotted resonant switch (a.k.a., resoswitch). Here, slots in the resoswitch structure that amplify displacement along a chosen axis similar to that of [1] are key to preventing input axis impacts that plagued a previous such power amplifying resonant switch [2]. In addition, the use of a low temperature Al surface-micromachining process to fabricate the switch allows this PA to be integrated directly over advanced CMOS. This work demonstrates for the first time RF power gain via a metal micromechanical displacement-amplifying resonant switch, and in doing so inches this technology towards not only the possibility of near 100% efficient power gain when used in a Class-E configuration [3] in RF transmitters, but also realization of a channel-selecting filter-LNA function that could substantially lower receive path power consumption.

### KEYWORDS

RF MEMS switch, resonant switch, resoswitch, RF channel selection, transceiver, aluminum.

### INTRODUCTION

The growing interest in long-lived, set-and-forget autonomous sensor networks, whereby wireless sensors are distributed with no intention of returning to replace their power sources, spurs an obvious need to minimize power consumption. Among components in a sensor node, the wireless communication module is very often a major power hog. Within this module, transmit power is critical, especially when sleep strategies are utilized to greatly reduce the average receive power consumption that might otherwise dominate the battery drain.

To minimize transmit power, the efficiency of the power amplifier (PA) is paramount. Among high efficiency PA topologies, the switched-mode Class-E design theoretically delivers the highest drain efficiency—ideally 100%—by shaping the switching waveform so that no power dissipates across the switch [3]. To date, however, the large parasitic capacitance associated with transistor-based switches limits the maximum frequency that allows an ideal Class-E waveform, thereby preventing actual Class-E PA's from reaching ideal efficiency [4].

When sleep strategies cannot be employed, e.g., in cellular networks, receive power can actually overshadow transmit energy consumption, since receive path electronics must remain "on" over periods to listen for interrogating signals. Thus, it is important that front-end RF receive path circuits, e.g., the low noise amplifier (LNA) and mixer, operate with very low standby power consumption.

Recent advances in MEMS technology that yield vibrating micromechanical resonant switches (a.k.a.

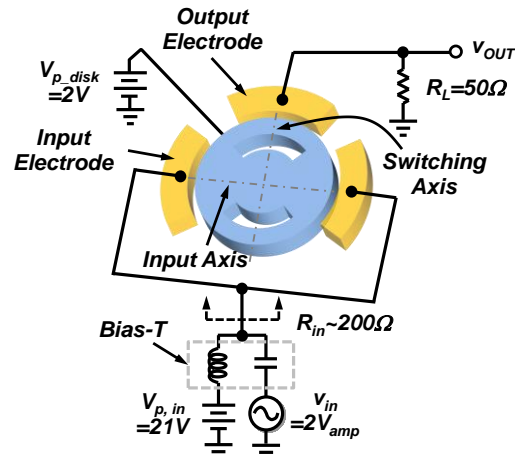


Fig. 1: Schematic of a slotted resoswitch in the simple switched-mode PA circuit used to attain 13.8 dB of power gain.

“resoswitches”) with substantially lower off capacitance than transistor switches, plus lower actuation voltage, higher speed, and better reliability than conventional RF MEMS switches, now offer a potential solution towards improved Class-E PA efficiency [1][2][5]. These devices are not only lucrative for transmit applications, but also receive, since they effectively behave as filter-LNA's. In particular, they first filter an incoming signal with channel-like selectivity, removing all blockers, thereby removing all nonlinearity-derived distortion [6]. This then permits switched-mode amplification by impact switching at the device output, all with zero quiescent power.

Unfortunately, the resoswitches demonstrated to date have been plagued with either high contact resistance (when constructed in polysilicon [1][2]), or added fabrication complexity [5] to achieve larger gap spacing along the input axis than the output axis in order to prevent impacting at the input port. To overcome these, this work uses aluminum metal structural material to realize a resoswitch equipped with displacement-amplifying slots that when embedded into an appropriate circuit (*cf.* Fig. 1) produces 13.8 dB of power gain.

### DEVICE STRUCTURE AND OPERATION

The Al displacement amplifying resoswitch of Fig. 1 essentially comprises a wine-glass mode disk resonator [7] with slots cut along one axis designed to lower the stiffness along this axis [1]. This then allows displacements along this (output switch) axis to be larger than those along the other (input) axis, in turn allowing the device to impact its electrodes along the output axis, but not along the input axis. The use of this displacement amplifying design obviates the need for added process complexity to create larger electrode-to-resonator gap spacings along the input axis than along the output, which was needed in an earlier rendition of a successful power amplifier [5].

To operate the device as a filter-power amplifier, i.e., filter-LNA, a supply voltage is first tied to the conductive

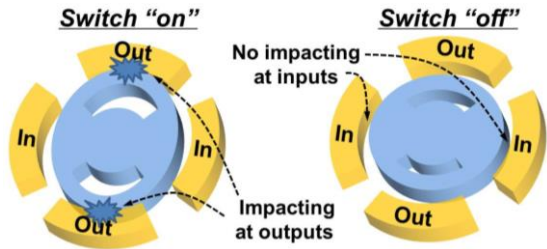


Fig. 2: Illustration of slotted resoswitch operation, showing impacting along the output axis, but not along the input axis.

**Conventional Disk Resonator      Displacement Amplifier**

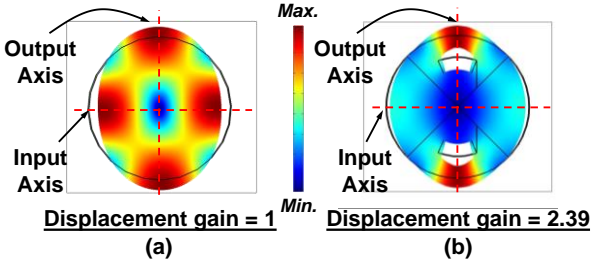


Fig. 3: FEM simulated mode shapes comparing displacements along input and output axes for (a) a wine-glass disk resonator and (b) a slotted displacement-amplifying resoswitch.

structure, and an input comprising a combined dc bias  $V_{P, input}$  and ac voltage  $v_{in}$  applied to the input electrodes. When the frequency of  $v_{in}$  is within a small bandwidth around the structure's resonance frequency, the structure begins to vibrate in the mode shape shown in Fig. 2, where it expands and contracts along its orthogonal input and output axes. Fig. 3 also includes the mode shape for a conventional un-slotted wine-glass disk in (a) for comparison. Note how the displacement amplitudes along the input and output axes are identical in (a) (for a gain = 1), whereas the slotted version in (b) exhibits a gain of 2.39.

If the magnitude of  $v_i$  is larger than a prescribed threshold, the signal drives the amplitude of vibration large enough to instigate impacting of the conducting resonator against its output electrodes. Since each impact closes a switch, this effectively switches the power supply to the output (periodically), thereby delivering power.

**FABRICATION PROCESS FLOW**

Fig. 4 presents the fabrication process flow used to achieve resoswitches in metal aluminum structural material. The process begins with the growth of 2- $\mu\text{m}$  thermal oxide on a starting silicon substrate, followed by atomic layer deposition (ALD) of 100-nm  $\text{Al}_2\text{O}_3$ , both of which together serve as electrical insulation. A 100-nm thick pure aluminum film is then sputtered and patterned via plasma etching, as shown in Fig. 4(a). Next, 750 nm of LPCVD oxide is deposited at 400°C to act as a sacrificial layer, followed by photolithography and etching to form anchors (Fig. 4(b)). Note that the 400°C deposition temperature is the lowest temperature limit of the deposition furnace and less than 2/3 of the Al melting point, chosen minimize impact on the first Al thin film. The second Al film (for the structure) is then sputtered 2.5- $\mu\text{m}$  thick, followed by deposition of a 1.5- $\mu\text{m}$ -thick oxide hard mask (Fig. 4(c)(d)). The electrode-to-resonator spacing is then defined by depositing a 70-nm sacrificial LPCVD oxide, again at 400°C, as seen in Fig. 4(e). The field oxide is then

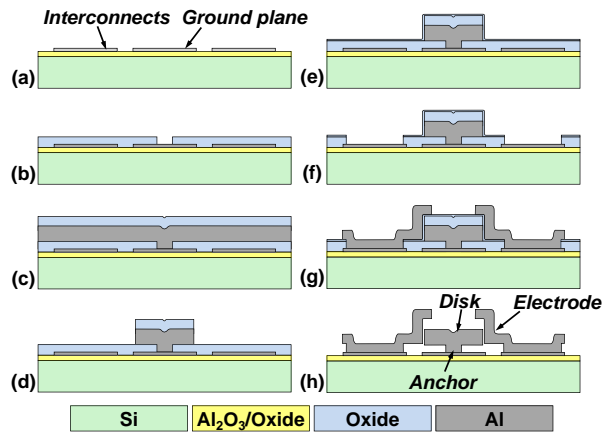


Fig. 4: Fabrication process flow used to achieve aluminum displacement amplifying resoswitches.

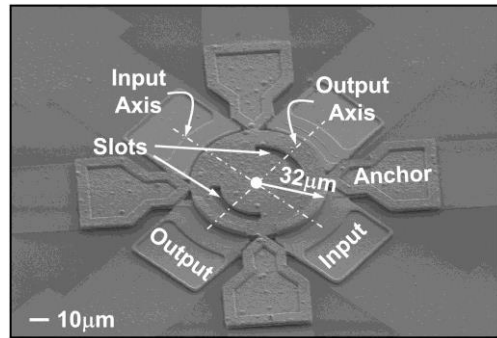


Fig. 5: SEM of a slotted displacement amplifying resoswitch is used to demonstrate power gain.

patterned to access interconnects (Fig. 4(f)), followed by a 1.5- $\mu\text{m}$  Al deposition, which is patterned to form electrodes (Fig. 4(g)). Finally, vapor phase HF removes all sacrificial oxide to yield Fig. 4(h). Due to vapor phase HF's very high oxide:Al selectivity, the Al structure remains intact after the release step. Fig. 5 presents the SEM of a fabricated Al slotted resoswitch.

**EXPERIMENTAL RESULTS**

**Displacement Gain**

The displacement gain of the slotted resoswitch was measured using the RF/LO mixing measurement setup introduced in [1] designed to simultaneously measure motional currents from any two ports on a capacitively transduced resonator. Fig. 6 presents the measured power waveforms generated at the electrodes of a resoswitch with 5- $\mu\text{m}$ -wide slots, clearly showing larger power from the output axis than the input. The equivalent displacement amplitude along each axis can then be extracted from measured output power as described in [1]. Doing so for Fig. 6 yields a displacement gain of 5.38 $\times$ , confirming the efficacy of slot-based stiffness engineering.

**Filter-PA Power Gain**

Fig. 7(a) presents the measured output waveform for the circuit of Fig. 1 using a slotted Al resoswitch. When  $v_{in} = 2$  V near the 23-MHz resonance frequency, the output displacement amplitude becomes large enough to impact the output electrode, thereby switching the  $V_{P, disk} = 2$  V supply to the output 50- $\Omega$  load to yield an output voltage amplitude of 0.15 V. When the input signal  $v_{in}$  is swept

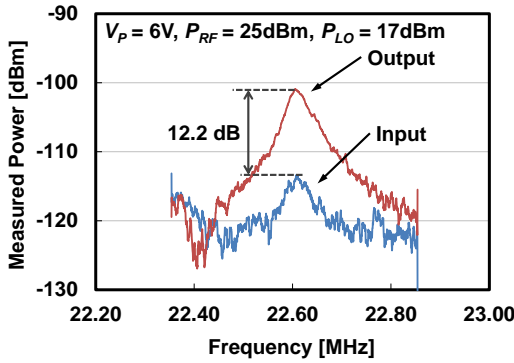


Fig. 6: Output power measured from input and output axes in a slotted Al resoswitch, revealing a displacement gain of 5.38.

over a frequency span around the resonance frequency, the resoswitch responds and produces output signals only over a small bandwidth around the resonance peak. For input signals outside this bandwidth, the switch is at rest, and there is no output. Thus, as advertised, the device performs both frequency selection and power amplification, as illustrated in Fig. 7(a).

Note that although there is no voltage gain, the input impedance of 200 k $\Omega$  determined by the device motional resistance is much higher than the output 50- $\Omega$  load, and thus, there is still a power gain of 13.8 dB as calculated in Fig. 7(b). This power gain lasted only a short while, since the device pulled into its electrode due the need for a rather large  $V_{p,in}$ , brought about by a device  $Q$  of only 500.

## UTILITY OF RESOSWITCHES

Having successfully demonstrated a displacement amplifying resoswitch, some discussion on the utility of this device for transmit and receive applications is useful.

### Switched-Mode Transmit PA

Fig. 8(a) presents a typical Class-E power amplifier utilizing a transistor switching device, along with equations in (b) that govern the inductor and capacitor values [3] needed to shape the waveforms so that ideally there is never current  $i_{switch}$  across the switch when the voltage  $v_D$  is not zero, cf. Fig. 8(c), in which case no power is wasted. The degree to which this ideal condition can be achieved is governed by whether or not the right element values are available, and this won't be the case if the switching device presents more "off" capacitance  $C_{off}$  at its drain node than the needed capacitance  $C_1$  at the desired frequency.

Table 1 compares typical characteristics for a conventional FET switch, a conventional RF MEMS switch, and the resoswitch of this work. Focusing for the moment on capacitance, while the  $C_{off} \sim 1.1$  pF for the GaN transistor switch in the table is much better than the  $\sim 20$  pF typical of CMOS counterparts, the MEMS switches are orders of magnitude better, with typical values under 10 fF. When embedded in a Class-E PA circuit as shown in Fig. 8(a), the smaller  $C_{off}$  of a MEMS resoswitch allows the use of ideal  $C_1$  at higher  $f_{max}$ , which means it better achieves a waveform where current and voltage are never simultaneously present in the switching device.

To better elucidate the resoswitch-induced benefits, Fig. 9 presents simulations of switch voltage and current in

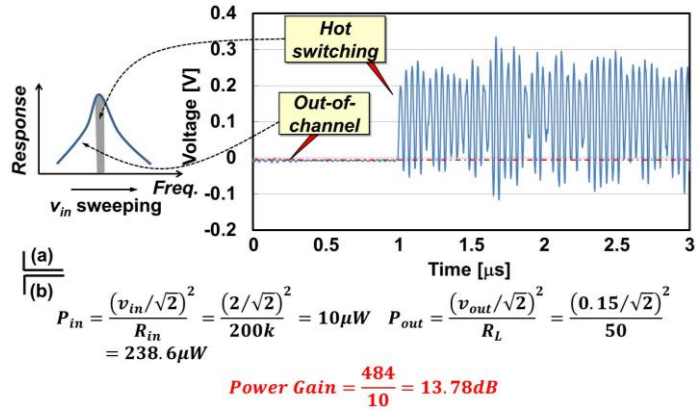


Fig. 7: (a) Measured output waveform for the circuit in Fig. 1 as the input frequency sweeps into the channel bandwidth. (b) Power gain calculations.

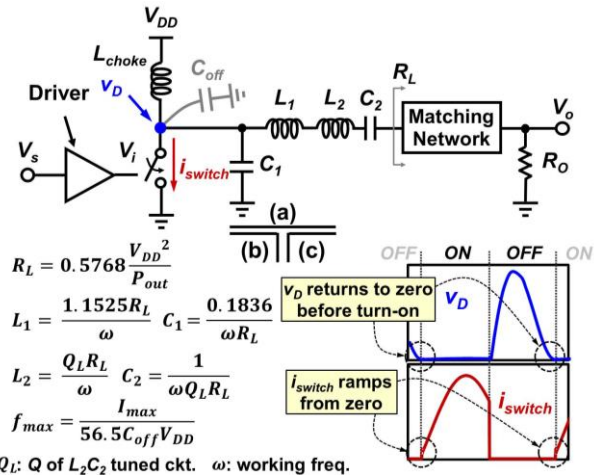


Fig. 8: (a) Schematic of a Class-E PA. (b) Equations governing the ideal LC component values. (c) Ideal non-overlapped switch voltage and current waveforms for zero power dissipation.

a typical Class-E PA for two cases: 1) a transistor switch with very large  $C_{off} \sim 1.1$  pF; and 2) a MEMS resoswitch that allows the right value of  $C_1$ . As expected, when  $C_1$  takes on the right value, very little energy per cycle is wasted. On the other hand, when  $C_{off} \sim 1.1$  pF, large currents spike during turn-on that dissipate sizable energy per cycle, thereby dramatically degrading efficiency. Clearly, if use of a resoswitch allows the right  $C_{off}$ , it should also greatly reduce transmit power consumption.

### Receive Path Filter-LNA

As covered in [6], if RF channel selection were available to remove all incoming blockers before they reach front-end electronics, then the local oscillator phase noise and dynamic ranges of the LNA and mixer in any RF front-end could be relaxed enormously, to the point where highly nonlinear (and thus, low power) designs of these functions become permissible.

As seen in Fig. 7(a), the resoswitch itself responds only over a small frequency bandwidth around its own resonance and rejects all other frequencies. In doing so, the device behaves as a very small percent bandwidth filter, i.e., a channel select filter, and it does its filtering before its amplification. In effect, the resoswitch realizes RF channel-selection and amplification, i.e., a filter-LNA function, in a single component, so stands to greatly alleviate the



Table 1: Switch Technology Comparison

	GaN HEMT Switch	Convl. MEMS Switch	Resoswitch
Actuation Voltage [V]	1-3	20-80	2
Switching Time	20-40 ns [8]	1-300 $\mu$ s	$\sim$ 10ns
Life Time (# cycles)	Very large	100 Billion	<sup>4</sup> 173 Trillion
Off State Current	28 $\mu$ A/mm [9]	0	0
$R_{on}$ [ $\Omega$ ]	1 [10]	0.1-1	0.5 [6]
$C_{off}$	<sup>1</sup> 1.1 pF [10]	1-10 fF	$\sim$ 7 fF
FOM ( $1/2\pi R_{on}C_{off}$ )	$\sim$ 145 GHz	$\sim$ 63 THz	$\sim$ 50 THz
<sup>2</sup> $f_{max}$ (Class-E PA)	514 MHz	<sup>3</sup> 113 GHz	80 GHz

1. Measured in an unpackaged bare die.  
 2. For a 10-W  $P_{out}$  with  $V_{DD} = 30V$ .  
 3. Which is not actually achievable due to slow switching speed.  
 4. For a polysilicon version.

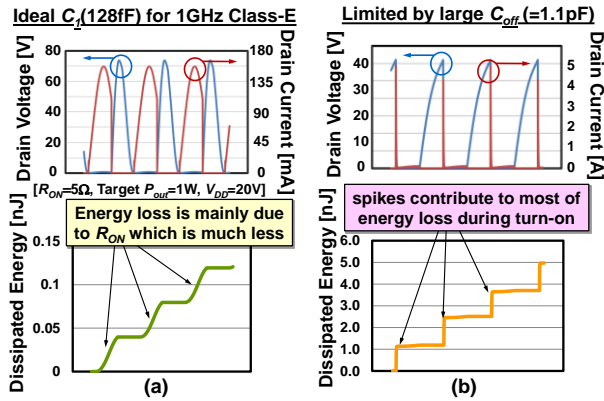


Fig. 9: Simulated Class-E waveforms using (a) the needed  $C_1$  and (b) a  $C_1$  limited by transistor drain parasitic capacitance, showing large energy loss due to non-ideal switching spikes caused by the larger-than-desired  $C_1$ .

design complexity of low-power RF receiver front-ends.

Of course, the input-to-output transfer function of this device is quite nonlinear, and normally this would be problematic, since it would allow blockers to generate spurious signals that could interfere with the desired signal. But this is of little consequence now that the filtering function of the resoswitch has removed all blockers, i.e., there are no blockers to generate intermodulation distortion or any other spurious signals. Furthermore, no dc current flows when the resoswitch is not resonating. Thus, this device consumes no quiescent power when in standby! With this device, the design of an FSK channel-select receiver with zero quiescent power might be as simple as that depicted in Fig. 10. The trick, of course, will be in how small the threshold voltage amplitude that instigates periodic switching can be made, as this governs sensitivity.

## CONCLUSIONS

Via use of aluminum structural material, the 23-MHz displacement amplifying resoswitch of this work greatly reduces its switch "on" resistance  $R_{ON}$  relative to previous polysilicon versions, thereby allowing power gains of up to 13.8 dB. By employing displacement amplifying slots, this design also eliminates the need for the oriented metal deposition process used in previous work to create different gap spacings along input and output axes. This demonstration fuels the exciting possibility of harnessing the channel-select filtering and nearly ideal switching functionalities of resoswitches to eventually attain transmit

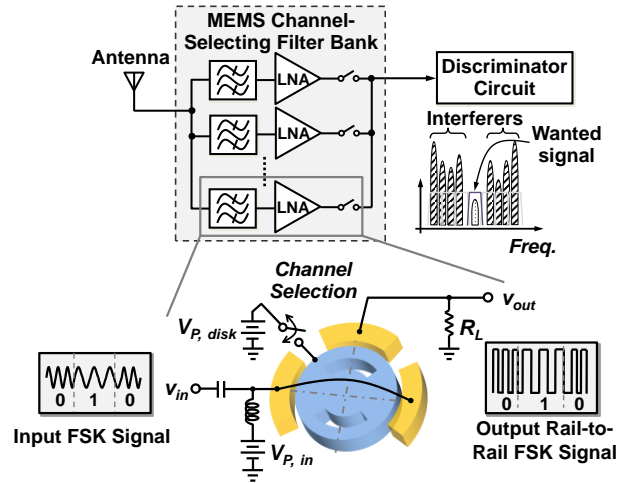


Fig. 10: Schematic of a low-power FSK receiver architecture using a bank of resoswitch filter-LNA's.

power amplifiers with unprecedented efficiency and receive filter-amplifiers with zero quiescent power consumption. Much work is of course needed before any of these become real, including contact and pull-in engineering to improve reliability, material and design adjustments to improve the device  $Q$ , and mechanical circuit design and control to better shape the device passband, all of which are the subject of ongoing research.

## ACKNOWLEDGEMENTS

The authors would like to thank Zeying Ren for valuable discussions and inputs on device fabrication. This work was supported by the DARPA NEMS program.

## REFERENCES

- [1] B. Kim, *et al.*, "Micromechanical Resonant ...," in *Proceedings*, 22nd Int. IEEE MEMS Conf., Sorrento, Italy, Jan. 25-29, 2009, pp.19-22.
- [2] Y. Lin, *et al.*, "The Micromechanical ...," in *Tech. Digest*, 2008 Solid-State Sen., Act., & Microsyst. Workshop, Hilton Head, SC, Jun. 1-5, 2008, pp. 40-43.
- [3] N. O. Sokal and A. D. Sokal, "Class E - A New ...," *IEEE J. Solid-State Circuits*, vol. 10, no. 3, pp. 168-176, 1975.
- [4] S. Lee, *et al.*, "Switching Behavior ...," *IEEE Trans. Microw. Theory Techn.*, vol. 60, no. 1, pp. 89-98, 2012.
- [5] Y. Lin, *et al.*, "A Metal ...," in *Tech. Digest*, IEEE Int. Electron Device Mtg., Washington, DC, Dec. 5-7, 2011, pp.20.6.1-20.6.4.
- [6] C. T.-C. Nguyen, "Frequency-Selective ...," *IEEE Trans. Microw. Theory Techn.*, vol. 47, no. 8, pp. 1486-1503, 1999.
- [7] Y.-W. Lin, *et al.*, "Series-Resonant VHF ...," *IEEE J. Solid-State*, vol. 39, no. 12, pp. 2477-2491, 2004.
- [8] "GaN Switches Enable Hot Switching at Higher Power," *Microwave Journal*, pp. 134-136, 2012.
- [9] Y. Cai, *et al.*, "High-Performance ...," *IEEE Electron Device Lett.*, vol. 26, no. 7, pp. 435-437, 2005.
- [10] "CGS60008D Datasheet," Rev 0.3, Cree, Inc., Apr. 2012.

## CONTACT

\*Wei-Chang Li, [wcli@eecs.berkeley.edu](mailto:wcli@eecs.berkeley.edu)